INORGANIC CHEMISTRY
FRONTIERS

RESEARCH ARTICLE

View Article Online
View Journal | View Issue



Cite this: *Inorg. Chem. Front.*, 2025, **12**, 3324

# 1,3-Dipolar cycloaddition reactions of triflatophosphanes to afford functionalized azaphospholium salts and azaphospholes†

Jannis Fidelius, [a] Kai Schwedtmann, [a] Sebastian Schellhammer, [b] Rongjuan Huang,[b] Felix Hennersdorf,[a] Moritz Fink, [a] Jan Haberstroh,[a] Antonio Bauzá, [c] Antonio Frontera, [c] Sebastian Reineke [b] and Jan J. Weigand *[a]

The advent of 1,3-dipolar cycloadditions in organic chemistry has introduced a powerful tool for constructing novel ring systems. However, methods for synthesizing inorganic, phosphorus-containing rings *via* 1,3-dipolar cycloadditions have remained scarce and are largely limited to the functionalization of phosphaalkynes. In this contribution, we describe the synthesis of 1,3-dipolar triflatophosphanes, demonstrating their ability to engage in (3 + 2)-cycloadditions with a variety of dipolarophiles. In addition to nitriles, (thio)-cyanates, iso-(thio)-cyanates, and (thio)-ketones, phosphaalkenes also exhibit reactivity, yielding a wide range of heteroatom-functionalized di- and triazaphospholium compounds. Density Functional Theory (DFT) calculations provide insight into the likely stepwise mechanism. Furthermore, the reduction of synthesized diazaphospholium salts affords neutral diazaphospholes, offering a novel route to this class of compounds. Importantly, we explored the photophysical properties of selected diazaphospholes that exhibit strong fluorescence with photoluminescence quantum yields of up to 37%, making them attractive candidates for applications in optoelectronics.

Received 12th February 2025,
Accepted 4th March 2025

DOI: 10.1039/d5qi00427f

rsc.li/frontiers-inorganic



## Introduction

1,3-Dipolar cycloaddition reactions are versatile and powerful tools in organic chemistry for the construction of heterocyclic ring systems with diverse structural motifs. These reactions involve the combination of a 1,3-dipolar compound with a suitable dipolarophile, resulting in the formation of novel ring structures. Among these, the (3 + 2)-cycloaddition, popularized by Huisgen[1] and extensively explored by many others, has gathered significant attention.[2] Two prominent variants of these "click" reactions are those of nitriles or alkynes with azides, leading to the formation of tri- or tetrazole derivatives.[3] Beyond azides, numerous other dipolarophiles, such as nitrile oxides[1] and diazoalkanes,[4] have been studied, resulting in a wide array of heterocyclic ring systems. A specific subfield of interest is the synthesis of heterocyclic compounds containing phosphorus atoms, which has attracted considerable attention due to their wide-ranging applications in fields such as materials science[5] and coordination chemistry.[6] However, only a limited number of (3 + 2)-cycloaddition reactions have been reported for the synthesis of phosphorus-containing heterocycles (see Scheme 1). In line with the classical click reactions of nitriles and azides (Scheme 1, I), Regitz first described the functionalization of phosphaalkynes **1** with azides to afford triazaphospholes **2** – a method that has been further explored by Müller and colleagues (Scheme 1, II).[7] Similarly, reactions with diazomethane derivatives yield diazaphospholes **3**.[8] Later, the same group demonstrated that diazaphospholes **4** could be obtained through analogue cycloadditions with azomethine ylides.[9] Nishibayashi described a copper-catalyzed variation of these cycloadditions, where phosphaalkynes **1** react with isocyanoacetates to form azaphospholes **5**.[10] Recently, Wolf and Hansmann showed that diazaphospholes and diazadiphosphholes could be obtained from the reaction of diazoalkenes with either phosphaalkynes **1** or $P_4$.[11]

In a remarkable reaction, the Cummins group demonstrated that *in situ*-formed phosphaethyne (H–C≡P) reacts with sodium azide to form the unsubstituted $[HCPN_3]^-$ anion.[12] In contrast to these results, few examples have been

[a]*Faculty of Chemistry and Food Chemistry, Technische Universität Dresden, 01062 Dresden, Germany. E-mail: jan.weigand@tu-dresden.de*
[b]*Dresden Integrated Center for Applied Physics and Photonic Materials (IAPP) and Institute of Applied Physics, Technische Universität Dresden, 01069 Dresden, Germany*
[c]*Department of Chemistry, Universitat de Illes Balears, 07122 Palma de Mallorca, Spain*

†Electronic supplementary information (ESI) available: Experimental procedures, analytical data and details on calculations. CCDC 2406453–2406470. For ESI and crystallographic data in CIF or other electronic format see DOI: https://doi.org/10.1039/d5qi00427f

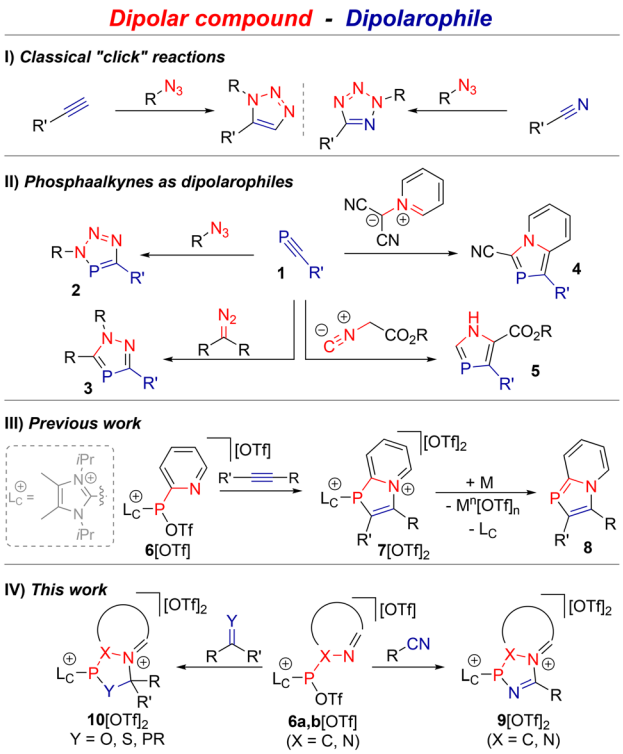


**Scheme 1** Synthetic approaches towards various heterocyclic ring systems; dipolar compounds are marked in red, dipolarophiles in blue. (I) Classical click reactions of alkynes or nitriles with azides; (II) diverse reactions of phosphaalkynes **1** to P/N-containing ring systems; (III) our previous work: dipolar imidazoliumyl-substituted triflatophosphanes reacting with alkynes to form azaphospholium salts, followed by subsequent reduction to 1,3-azaphospholes; (IV) the present work: expansion of our dipolar cycloaddition methodology with different compounds featuring carbon–heteroatom multiple bonds.

reported where the 1,3-dipolar compound, rather than the dipolarophile, features the phosphorus atom. One such example was recently described by our group, wherein 1,3-dipolar fluorophosphonium compounds react with small molecules to form novel ring systems.[13] Additionally, Streubel reported on the *in situ* preparation of nitrilium phosphaneylide tungsten complexes, which react with alkynes to afford 1,2-azaphosphole tungsten complexes.[14]

Recently, our group has reported on dipolar cycloadditions involving imidazoliumyl-substituted triflatophosphanes **6**[OTf], which react with alkynes to form azaphospholium salts **7**$[OTf]_2$. These salts can be readily reduced to yield neutral azaphospholes **8** (Scheme 1, III), providing a novel approach for accessing this class of compounds.[15] With this background in mind, we sought to explore the potential of our cycloaddition method with other dipolarophiles.

In this study, we expand our methodology to construct novel phosphorus-containing ring systems: triflatophosphanes, like **6**[OTf], were found to react with nitriles and various other dipolarophiles, resulting in the formation of (poly)-azaphospholium salts of the type **9**$[OTf]_2$. These compounds hold great potential for reduction to their neutral phosphole counterparts, as demonstrated by the reduction of a model compound. Additionally, reactions involving compounds with carbon–heteroatom double bonds were found to yield partially saturated heterophospholium salts **10**$[OTf]_2$.

## Results and discussion

### 1,3-Dipolar cycloaddition reactions with CN triple bonds

The formation of dipolar triflatophosphane **6**[OTf] was achieved by reacting chlorophosphane **11**[OTf] with silver triflate (AgOTf).[15] Due to the limited stability of **6**[OTf], we employed our *in situ* generation approach for this salt in the presence of the dipolarophile. Upon the addition of AgOTf to **11**[OTf] in acetonitrile, a new signal emerged in the $^{31}P$ NMR spectrum of the reaction solution at $\delta(P) = 21.6$ ppm, indicating a clean cyclization reaction to diazaphospholium salt **9a**$[OTf]_2$ (see Scheme 2).

After filtration and removal of the solvent, **9a**$[OTf]_2$ was isolated in good yield of 81% as an analytically pure, colourless solid. Single crystals obtained from a saturated solution of **9a**$[OTf]_2$, were analyzed by single-crystal X-ray diffraction (SC-XRD). The molecular structure of **9a**$[OTf]_2$ is depicted in Fig. 1, confirming the structural connectivity. The molecular structure of **9a**$[OTf]_2$ reveals the expected distorted pyramidal bonding environment at the phosphorus atom. The P–C bond (1.8145(13) Å) is comparable to other known examples of imidazoliumyl-substituted phosphanes.[16] While the imidazoliumyl fragment remains planar, the diazaphospholium moiety exhibits slight distortion, as evidenced by a torsion angle N2–C2–P1–N1 of 13.20(9)°. A limited π-electron delocalization in the diazaphospholium moiety is furthermore indicated by the N1═C3 bond length (1.2689(19) Å), characteristic of a C═N

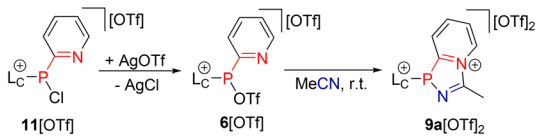


**Scheme 2** Reaction of *in situ* prepared **6**[OTf] with acetonitrile to afford diazaphospholium salt **9a**$[OTf]_2$.

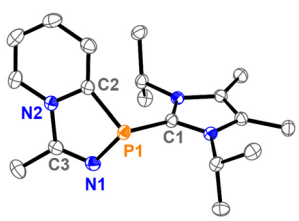


**Fig. 1** Molecular structure of $\mathbf{9a}^{2+}$ in **9a**$[OTf]_2$ (hydrogen atoms and counter ions are omitted for clarity; thermal ellipsoids are displayed at 50% probability). Selected bond lengths in Å and angles in (°): P1–C1 1.8145(13), P1–N1 1.7122(12), P1–C2 1.8199(14), N1–C3 1.2689(19), C3–N2 1.4606(18), N1–P1–C1 105.27(6), N1–P1–C2 91.72(6), C1–P1–C2 107.50(6), N2–C2–P1–N1 13.20(9).

double bond. In subsequent experiments, selected nitriles with different functional groups were used as substrates for the formation of diazaphospholium compounds **9a–f**[OTf]$_2$. The reaction yields and $^{31}$P NMR shifts are summarized in Scheme 3.

By elevating the reaction temperature to 40 °C, the reaction time for derivatives **9a–f**[OTf] was significantly reduced. After workup, **9a–f**[OTf]$_2$ were obtained as colourless or red (**9e**[OTf]$_2$) powders in moderate to excellent yields. Notably, the reactions afforded not only the simple methyl-substituted compound **9a**[OTf]$_2$ but also electron-deficient (**9c**[OTf]$_2$) and electron-rich (**9e**[OTf]$_2$) derivatives, with no significant changes in yields. However, in the reaction with propionitrile (yielding **9b**[OTf]$_2$), no increase in the yield could be achieved, likely due to the limited reactivity of propionitrile. Furthermore, when 1,4-phenyldiacetonitrile was used, the bridged derivative **9f**[OTf]$_4$ was obtained. The diazaphospholium compounds show $^{31}$P NMR chemical shifts between $\delta$(P) = 21.6 to 27.7 ppm. Single crystals of most derivatives were obtained by the slow diffusion of $Et_2O$ into saturated MeCN solutions **9a–f**[OTf]$_2$. The molecular structures are given in the ESI (section 2.3†).

The bonding parameters were found to be comparable to those observed for **9a**$^{2+}$, regardless of the steric or electronic properties of the substituents.

To further expand the scope of the cycloadditions, **6**[OTf] was reacted with phenylcyanate. The $^{31}$P NMR spectrum of the reaction solution revealed the formation of a new compound with a resonance at $\delta$(P) = 14.5 ppm, slightly upfield-shifted compared to that of **9**[OTf]$_2$. Filtration and solvent evaporation yielded **12**[OTf]$_2$ in an excellent yield of 87%. When the same reaction was conducted using ethylthiocyanate, **13**[OTf]$_2$ was obtained in 85% yield (see Scheme 4). The $^{31}$P chemical shift of **13**[OTf]$_2$ ($\delta$(P) = 27.9 ppm) is similar to those of diazaphospholium salts **9**[OTf]$_2$ (*vide supra*).

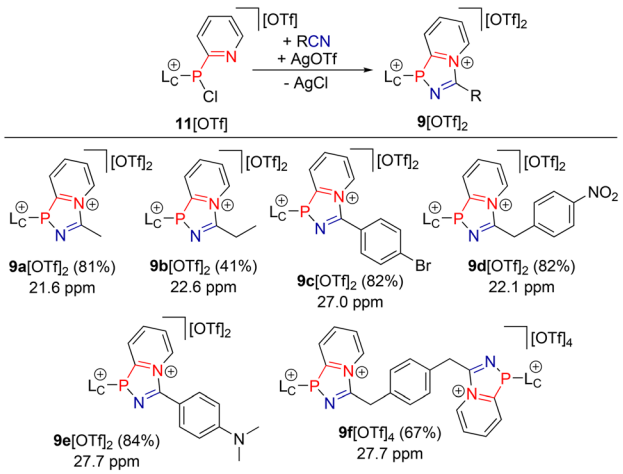


**Scheme 3** Syntheses of **9a–e**[OTf]$_2$ and **9f**[OTf]$_4$ through reactions of *in situ* prepared **6**[OTf] with various nitriles; $^{31}$P NMR chemical shift in ppm and yield in %.

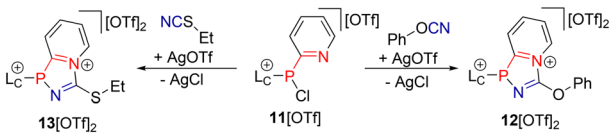


**Scheme 4** Syntheses of **12**[OTf]$_2$ and **13**[OTf]$_2$ through the cycloaddition of *in situ* formed **6**[OTf]$_2$ with ethylthiocyanate or phenylcyanate.

Single crystals of **12**[OTf]$_2$ were obtained by the slow diffusion of $Et_2O$ into a solution of **12**[OTf]$_2$ in $CH_2Cl_2$. The molecular structure of **12**$^{2+}$ is depicted in Fig. 2, and in comparison with **9a**$^{2+}$, the C1–P1 (**12**$^{2+}$: 1.8263(14) Å; **9a**$^{2+}$: 1.8145 (13) Å) and the P1–N1 (**12**$^{2+}$: 1.7125(13) Å; **9a**$^{2+}$: 1.7122(12) Å) bond lengths are similar. However, an elongation of the P1–C2 (**12**$^{2+}$: 1.8402(14) Å; **9a**$^{2+}$: 1.8199(14) Å) and a contraction of the N2–C3 (**12**$^{2+}$: 1.4444(18) Å; **9a**$^{2+}$: 1.4606(18) Å) bond lengths are observed. The C3–O1 (1.3212(18) Å) bond length in **12**$^{2+}$ is considerably shorter than the O1–C4 (1.4167(17) Å) bond length, indicating delocalization involving the free lone pairs of the oxygen atom, consistent with the high-field shift observed in the $^{31}$P NMR spectrum.

## Chemical reductions of the diazaphospholium salts

In our previous work, we demonstrated the reduction of related azaphospholium salts to neutral azaphospholes under elimination of the parent NHC (see Scheme 1).[15] Building on this, we investigated the reduction of diazaphospholium salt **9a**[OTf]$_2$ as a model compound, aiming to establish a convenient pathway for synthesizing a wide range of diazaphospholes.

In order to gain a deeper understanding of its electrochemical reactivity, **9a**[OTf]$_2$ was subjected to electrochemical studies, including cyclic voltammetry (CV) and square wave voltammetry (SWV). The CV of **9a**[OTf]$_2$ in $CH_2Cl_2$ revealed a non-reversible reduction with a peak potential (CV) of $E_p$ = −0.86 V and a SWV formal potential of $E$ = −0.80 V (*vs.* $E_{1/2}(Cp_2Fe/Cp_2Fe^+)$). Further details are provided in the ESI.† Subsequently, we investigated the chemical reduction of

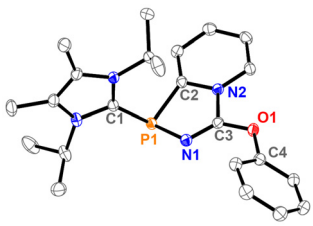


**Fig. 2** Molecular structure of **12**$^{2+}$ in **12**[OTf]$_2$ (hydrogen atoms and counter ions are omitted for clarity; thermal ellipsoids are displayed at 50% probability). Selected bond lengths in Å and angles in (°): P1–C1 1.8263(14), P1–N1 1.7125(13), P1–C2 1.8402(14), N1–C3 1.2643(19), C3–N2 1.4444(18), C3–O1 1.3212(18), O1–C4 1.4167(17), N1–P1–C1 104.00(6), N1–P1–C2 91.73(6), C1–P1–C2 107.69(6), N2–C2–P1–N1 12.16(10).

**9a**[OTf]$_2$, using potassium graphite ($KC_8$) as a reducing agent. Upon suspending a mixture of two equivalents of $KC_8$ and **9a**[OTf]$_2$ in THF at −78 °C, the clean formation of the neutral diazaphosphole **14** was observed, indicated by a new resonance in the $^{31}$P NMR spectrum of the reaction mixture with a chemical shift of $\delta$(P) = 150.4 ppm. After the removal of K[OTf] and NHC **15**, **14** was isolated in 62% yield as a yellow crystalline solid (see Scheme 5). In order to gain further understanding of the influence that annulation and substitution have on the properties of these phospholes, we synthesized compounds **16** and **17** from the respective crude diazaphospholium salts **9g**[OTf]$_2$ and **31**[OTf]$_2$ (see Scheme 5). This demonstrates that, using our synthetic method, a similar range of derivatives is accessible as for the previously described 1,3-azaphospholes **8**.

It should be noted, however, that the reductions of **12**[OTf]$_2$ and **13**[OTf]$_2$ only resulted in the formation of trace amounts of the respective diazaphospholes (>10%); thus, we concluded that the bulk synthesis might not be suitable for this study. Single crystals of **16** were analysed with X-ray diffraction, and the molecular structure is depicted in Fig. 3. As expected, the overall bond lengths in the five-membered diazaphosphole ring are shortened (P1–N1 1.6883(18) Å, P1–C1 1.735(2) Å) compared to **9a**$^{2+}$ (P1–N1 1.7122(12) Å, P1–C2 1.8199(14) Å), reflecting an increased aromatic character. Additionally, the structural parameters of **16** are similar to those observed for the corresponding azaphosphole **8** (R = Ph and R′ = H).[15]

## Characterization of diazaphospholes 14, 16, and 17

To gain further insights into the electronic structures and photophysical properties of diazaphospholes **14**, **16**, and **17**, we conducted quantum chemical simulations and spectroscopic measurements, similar to our recent studies of azaphospholes **8**.[15] The key characteristics are summarized in Table S1.† Both molecules **8** (R = Me, R′ = H) and **14** exhibit similar characteristics regarding their frontier molecular orbitals, aromaticity, and absorption/emission properties. Notably, the second nitrogen atom in the diazaphospholes stabilizes both the HOMO and LUMO by approximately 300 meV (Fig. 4a). Both HOMO and LUMO can be slightly shifted towards the gap through pronounced delocalization, as observed for **16**, where the substitution of a phenyl group at the C2 position enhances this effect. For **17**, benzannulation further increases this delocalization. This latter strategy results in the strongest modification of the aromaticity, as depicted in Fig. S114 in the ESI.† In general, both rings within **14** exhibit substantial aromatic character, as indicated by low nucleus-independent chemical shifts (NICS(1)$_{zz}$) values of −36.4 for the five-membered ring and −15.6 for the six-membered ring, respectively. These values are similar to those observed for 1,3-azaphospholes **8** and also correlate with the observations made by Dostál *et al.* for 1,2-azaphospholes.[15,17] The high degree of aromaticity in **14** is further supported by the anisotropy of the induced current density (ACID) plot, which reveals the delocalization of electron density across the bicyclic

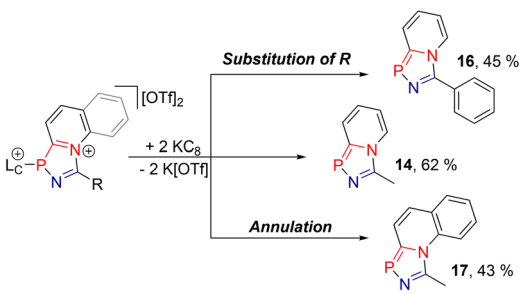


**Scheme 5** Reduction of diazaphospholium salts **9a**[OTf]$_2$, **9g**[OTf]$_2$ and **18**[OTf]$_2$ to neutral diazaphosphole **14**, with the elimination of NHC **15**.

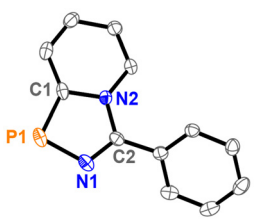


**Fig. 3** Molecular structure of **16** (hydrogen atoms are omitted for clarity; thermal ellipsoids are displayed at 50% probability). Selected bond lengths in Å and angles in (°): P1–C1 1.735(2), P1–N1 1.6883(18), C1–N2 1.404(2), N1–C2 1.310(3), C2–N2 1.387(3), N1–P1–C1 91.68(10), N1–C2–N2 115.21(16), C2–N1–P1–C1 0.91(19).

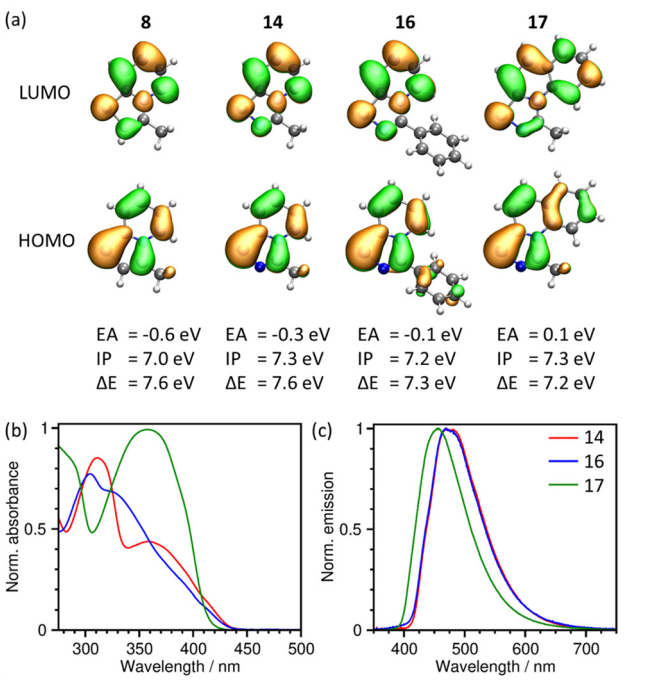


**Fig. 4** Electronic structure and photophysical properties of **14**, **16**, and **17** (5 wt% in a PMMA film). (a) Frontier molecular orbitals and the corresponding energies in a vacuum (CAM-B3LYP/6-311G**). (b) Normalized absorption spectra relative to the absorption maximum of **17**. (c) Normalized emission spectra ($\lambda_{exc}$ = 340 nm).

system. Although **16** shows a light decrease in aromaticity due to a pronounced delocalization of the electron density, benzannulation in **17** introduces another aromatic ring ($NICS(1)_{zz}$ = −27.5), though this reduces the aromaticity of the central ring ($NICS(1)_{zz}$ = −7.0).

Regarding their photophysical properties, the absorption and emission spectra of **14**, **16**, and **17** were recorded in chloroform (see Fig. S26†) and PMMA films at room temperature (Fig. 4b and c). In PMMA, diazaphosphole **14** shows two absorption peaks at 310 nm and 360 nm. In chloroform, the high-energy absorption peak splits into two absorption features. However, time-dependent density functional theory (TD-DFT, CAM-B3LYP/6-311G**) calculations show that this results from the electronic transition $S_0 \rightarrow S_2$. The simulated spectra depicted in Fig. S115† support the experimental observations well. While the absorption spectra of **16** show strong similarities in both chloroform and PMMA film compared to **14**, **17** reveals a pronounced absorption coefficient for the $S_0 \rightarrow S_1$ transition around 350 nm.

In our previous study on 1,3-azaphospholes **8**, room temperature phosphorescence (RTP) was observed for several derivatives.[15] However, no such features were obtained for diazaphospholes **14**, **16**, and **17**. These compounds show fluorescence with peaks in the range of 450 and 480 nm in PMMA (see Fig. 4c) similar to the fluorescence observed for previous 1,3-azaphospholes **8**. The photoluminescence quantum yield ($\Phi$) is significantly increased for diazaphospholes. Compound **14** shows superior results, with a quantum yield of 33.1% in chloroform and 37.0% in PMMA film (see ESI section 4†).

### 1,3-Dipolar cycloaddition reactions with carbon–heteroatom double bonds

Next, we aimed to explore the potential of reacting triflatophosphane **6**[OTf] with various compounds containing carbon-heteroatom or carbon–carbon double bonds (Scheme 6). Initially, we tested reactions of **6**[OTf] with alkenes and imines, similar to the other cycloaddition reactions described herein, but no reactions were observed. A comprehensive list of investigated dipolarophiles is provided in ESI section 2.7.†

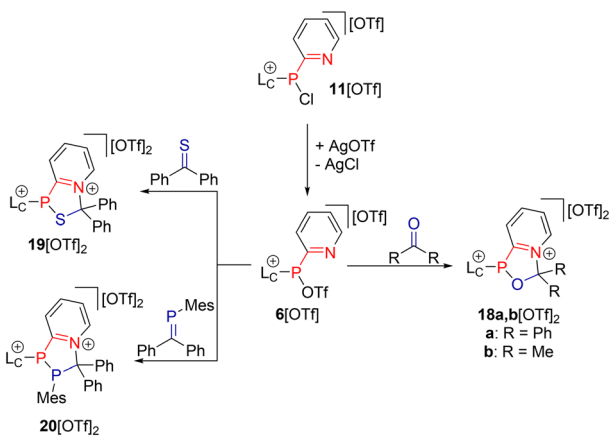


**Scheme 6** Reactions of *in situ* prepared **6**[OTf] with dipolarophiles containing carbon–heteroatom double bonds.

Upon addition of one equivalent of benzophenone to a solution of *in situ* prepared **6**[OTf], the clean formation of the unusual oxazaphospholium salt **18a**$[OTf]_2$ was observed, marked by a broad resonance in the $^{31}P$ NMR spectrum of the reaction mixture at $\delta(P)$ = 65.8 ppm. After filtration and solvent removal, **18a**$[OTf]_2$ was isolated in 76% yield as a colourless solid.

When **6**[OTf] was reacted with acetone, the oxazaphosphole **18b**$[OTf]_2$ was obtained in 25% yield. The relatively low yield of **18b**$[OTf]_2$ can be attributed to the formation of side products, which were removed by several recrystallizations. However, when a thioketone such as thiobenzophenone is used, the thiazaphospholium salt **19**$[OTf]_2$ was obtained in 87% yield. Notably, reactions with carbonyl and thiocarbonyl compounds proved much faster than cycloadditions with nitriles, reaching full conversion in a matter of minutes. In comparison with **18a,b**$[OTf]_2$ (**18a**$[OTf]_2$: $\delta(P)$ = 65.8 ppm; **18b**$[OTf]_2$: $\delta(P)$ = 71.8 ppm), **19**$[OTf]_2$ exhibits a considerably high-field shifted resonance in the $^{31}P$ NMR spectrum at $\delta(P)$ = −15.1 ppm, likely due to the presence of a neighbouring sulfur atom. Using the $MesP{=}CPh_2$ phosphaalkene[18] as the dipolarophile, we successfully obtained the unusual azadiphospholium salt **20**$[OTf]_2$ in an excellent yield of 88%. The $^{31}P$ NMR spectrum of **20**$[OTf]_2$ shows two resonances as an AM spin system, with chemical shifts of $\delta(P_A)$ = −51.0 ppm and $\delta(P_M)$ = 29.7 ppm. The moderate $^1J_{PP}$ coupling constant of −170 Hz is attributed to the *trans*-orientation of the two neighbouring phosphorus atoms, leading to minimal interaction between their free electron pairs – a phenomenon well-documented in polyphosphanes.[19]

Surprisingly, we found that **20**$[OTf]_2$ is unstable in MeCN solutions, slowly converting into compound **9a**[OTf] with the release of $MesP{=}CPh_2$. This slow reaction reached approximately 50% conversion after 10 days, with a reaction rate constant ($k'$) of $9.29 \times 10^{-7}$ $s^{-1}$ (see ESI section 2.7†).

We obtained X-ray quality crystals of compounds **18a**$[OTf]_2$, **19**$[OTf]_2$, and **20**$[OTf]_2$ for SC-XRD analysis. The molecular structures are depicted in Fig. 5. As expected, all three compounds exhibited a distorted pyramidal bonding environment around the central phosphorus atom. The P1–C1 bond lengths (**18a**$^{2+}$: 1.8835(15) Å, **19**$^{2+}$: 1.8245(12) Å, **20**$^{2+}$: 1.8300(18) Å) are within the expected range for imidazoliumyl-substituted phosphanes, similar to those observed for **9a**$^{2+}$. However, **18a**$^{2+}$ shows a slight elongation of the P1–C1 bond, indicative of higher electron density at the phosphorus atom, likely due to a +M effect of the oxygen atom influencing the phosphole ring. The overall planarity of the azaphospholium moiety varied significantly between the compounds. While **18a**$^{2+}$ is near planar (torsion angle N1–C2–P1–O1 10.14(10)°), **19**$^{2+}$ (N1–C2–P1–S1 27.41(8)°) and **20**$^{2+}$ (N1–C2–P1–P2 30.00(9)) display substantial distortions. The elongation of the P2–C3 bond in **20**$^{2+}$ (1.9610 (17) Å) is likely due to steric repulsion between the mesityl substituent and the two phenyl groups. For comparison with the diazaphospholium salt **9a**$[OTf]_2$, we have also investigated the reduction of **18a**$[OTf]_2$, **19**$[OTf]_2$ and **20**$[OTf]_2$ with two equiva-

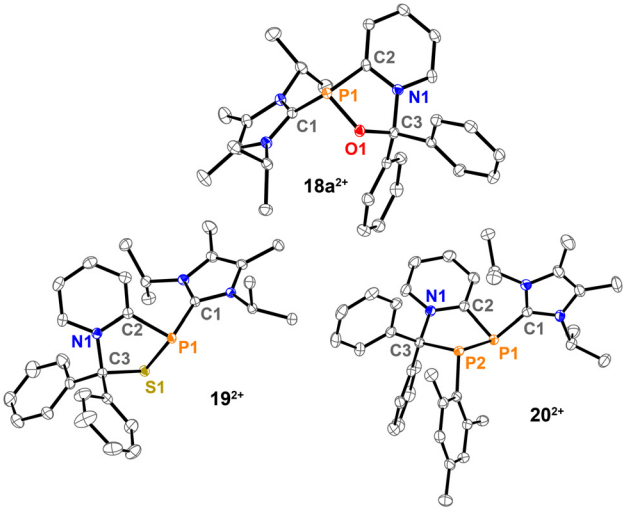


**Fig. 5** Molecular structures of **18a**$^{2+}$ in **18a**[OTf]$_2$·$CH_2Cl_2$, **19**$^{2+}$ in **19**[OTf]$_2$ and **20**$^{2+}$ in **20**[OTf]$_2$·$2C_2H_4Cl_2$ (hydrogen atoms, solvent molecules, and counter ions are omitted for clarity; thermal ellipsoids are displayed at 50% probability). Selected bond lengths in Å and angles in (°): **18a**$^{2+}$: C1–P1 1.8835(15), P1–O1 1.6651(11), P1–C2 1.8413(14), C2–N1 1.3555(19), N1–C3 1.5230(17), O1–C3 1.4246(16), C1–P1–O1 102.49(6), C1–P1–C2 104.48(6), C2–P1–O1 88.43(6), N1–C2–P1–O1 10.14(10); **19**$^{2+}$: C1–P1 1.8245(12), P1–S1 2.1328(5), P1–C2 1.8391(13), C2–N1 1.3553(16), N1–C3 1.5300(15), S1–C3 1.8393(13), C1–P1–S1 104.29(4), C1–P1–C2 98.44(5), C2–P1–S1 90.20(4), N1–C2–P1–S1 27.41(8); **20**$^{2+}$: C1–P1 1.8300(18), P1–P2 2.2137(6), P1–C2 1.8322(18), C2–N1 1.358(2), N1–C3 1.514(2), P2–C3 1.9610(17), C1–P1–P2 106.01(6), C1–P1–C2 97.98(8), P2–P1–C2 88.98(6), N1–C2–P1–P2 30.00(9).

lents of $KC_8$, all resulting in the decomposition of the starting material.

### Alteration of the N-donor substituent

Given the favourable applicability of our methodology, we sought to synthesize phospholium salts featuring a P–N bond in the nucleophilic moiety, based on previously reported pyrazolyl-substituted derivatives,[20,21] enabling post-functionalization. Initially, we encountered challenges in the synthesis of **21**[OTf], primarily due to rapid scrambling reactions, which led to the formation of dichloro-substituted compound **22**[OTf] and dipyrazolyl-substituted compound **23**[OTf], as outlined in Scheme 7. It was observed that an equilibrium between these three compounds rapidly formed in solution (see Fig. S1†). Additional details regarding the proposed mechanism and experiments are provided in the ESI.† Consequently, for the synthesis of the reactive species for 1,3-dipolar cycloaddition reactions, we employed a comproportionation approach. The addition of two equivalents of AgOTf to a mixture of **22**[OTf] and **23**[OTf] in $CH_2Cl_2$ led to the formation of two new resonances in the $^{31}$P NMR spectrum at $\delta$(P) = 86.4 ppm and 34.7 ppm, corresponding to a dynamic equilibrium between triflatophosphane **24**[OTf] and its dimer, the cyclic compound **25**[OTf]$_4$ (Scheme 7).

Variable-temperature $^{31}$P NMR experiments revealed a reversible increase in the integration of the low-field resonance

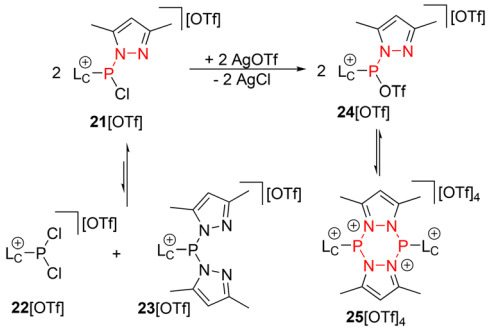


**Scheme 7** Synthesis of **21**[OTf] through a comproportionation reaction of **22**[OTf] and **23**[OTf], followed by the addition of AgOTf, resulting in an equilibrium between **24**[OTf] and its dimeric form, **25**[OTf]$_4$.

at $\delta$(P) = 86.4 ppm, attributed to triflatophosphane **24**[OTf] (see ESI section 2†). This finding suggests that the dimerization of **24**$^{2+}$ in solution stabilizes the highly electrophilic phosphorus atom, resulting in the formation of dimer **25**$^{4+}$, similar to previous observations.[15] The equilibrium was confirmed by two correlation peaks observed in the corresponding $^{31}$P–$^{31}$P-EXSY NMR experiment (Fig. S4†).

Single crystals suitable for X-ray analysis were obtained by the slow diffusion of *n*-pentane into a saturated $CH_2Cl_2$ solution of **24**[OTf] at −30 °C. The molecular structure of **24**$^+$ shows the coordination of one triflate anion to the electrophilic phosphorus atom, confirming the formation of triflatophosphane **24**$^+$ (see Fig. 6). A pyramidal bonding environment around the phosphorus atom is observed, with the P–O bond length (P1–O1: 1.7250(11) Å) being significantly shorter than those in other triflatophosphanes, indicating a strong covalent character.[22] This is supported by the elongation of the O–S bond (1.5540(11) Å) compared to the free triflate anion (av. 1.4314 Å). The P–C bond (**24**$^+$: 1.8229(6) Å; **23**$^+$: 1.8438(13) Å (ref. 20)) and the P–N bond (**24**$^+$: 1.6927(13) Å; **23**$^+$: 1.7171(11) Å (ref. 20)) are both shortened, indicating the high electrophilicity of the phosphorus atom.

Upon dissolving **24**[OTf] in acetonitrile, a new resonance of the cycloaddition product, triazaphospholium salt **26a**[OTf]$_2$, appeared in the $^{31}$P NMR spectrum at $\delta$(P) = 62.7 ppm. After filtration and drying *in vacuo*, **26a**[OTf]$_2$ was isolated in a good

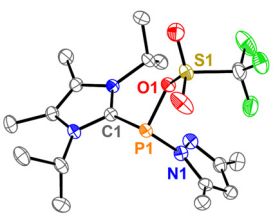


**Fig. 6** Molecular structure of cation **24**$^+$ in **24**[OTf]·$CH_2Cl_2$ (hydrogen atoms, solvate molecules, and anions are omitted for clarity; thermal ellipsoids are displayed at 50% probability). Selected bond lengths in Å and angles in (°): P1–C1 1.8229(15), P1–O1 1.7250 (11), P1–N1 1.6927 (13), C1–P1–N1 99.73(6), C1–P1–O1 96.81(6), O1–P1–N1 100.52(6).

yield of 82%. The key to this successful synthesis was to first achieve the *in situ* formation of **24**[OTf] in a three-component reaction from **22**[OTf], **23**[OTf], and AgOTf, followed by removal of the AgCl by-product and the subsequent addition of acetonitrile. Using this optimized method, we isolated the same range of derivatives previously described for **9**$[OTf]_2$ (Scheme 8). The yields were consistent, with most derivatives being isolated in approximately 80% yield. The reaction with propionitrile gave **26b**$[OTf]_2$ in lower amounts, due to lower reactivity, as observed previously for **9b**$[OTf]_2$. Additionally, both electron-rich (**26e**$[OTf]_2$) and electron-poor (**26c,d**$[OTf]_2$) derivatives are accessible.

The molecular structures of most of the derivatives were determined *via* SC-XRD analysis. However, due to similarities in the core unit, we focus here on the discussion of **26a**$[OTf]_2$. The molecular structure of $\mathbf{26a}^{2+}$ (Fig. 7) reveals the expected distorted pyramidal bonding environment around the central phosphorus atom.

The P–C bond (1.8306(16) Å) is comparable to other imidazoliumyl-substituted phosphanes.[16] While the pyrazolium fragment is planar, the five-membered triazaphosphole ring shows slight distortion (torsion angles in (°): N2–P1–N1–C2 8.46(12)), as is typical for such compounds.[23] The low degree of π-electron delocalization in the triazaphosphole moiety is further highlighted by the bond lengths within the ring fragments. The P1–N2 bond (1.7757(14) Å) is elongated compared to $\mathbf{23}^{+}$ (1.7171(11) Å (ref. 20)), while the pyrazolylium fragment appears aromatic. The N1=C2 bond (1.277(2) Å) is consistent with a typical N=C double bond. It should be noted that reductions, similar to that of **9a**$[OTf]_2$ were unfortunately unsuccessful for **26a**$[OTf]_2$.

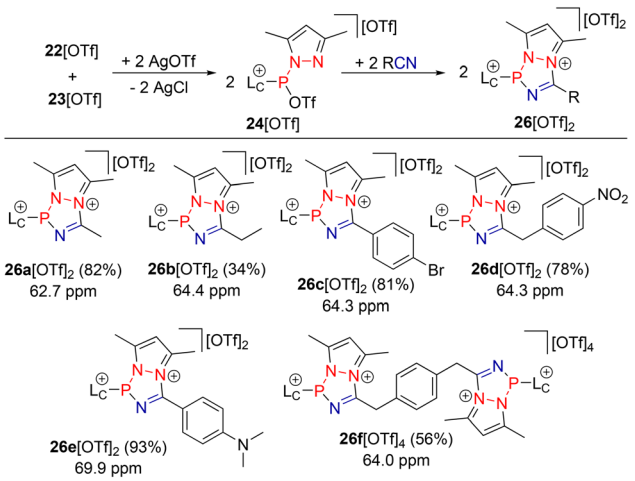


**Scheme 8** Syntheses of triazaphospholes **26a–f**$[OTf]_2$ through the cycloaddition of **23**[OTf] with various nitriles; $^{31}P$ NMR chemical shift in ppm, yield in %.

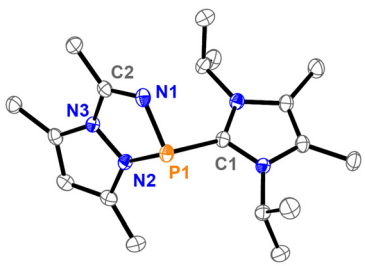


**Fig. 7** Molecular structure of cation $\mathbf{26a}^{2+}$ in **26a**$[OTf]_2 \cdot CH_2Cl_2$ (hydrogen atoms, solvate molecules, and anions are omitted for clarity; thermal ellipsoids are displayed at 50% probability). Selected bond lengths in Å and angles in (°): P1–C1 1.8306(16), P1–N1 1.7002(14), P1–N2 1.7757(14), N1–C2 1.277(2), C2–N3 1.427(2), N1–P1–N2 90.10(7), N1–P1–C1 102.66(7), C1–P1–N2 102.60(7), N2–P1–N1–C2 8.46(12).

## Mechanistic insights

Given the significant polarization of the C≡N triple bond in nitriles, we aimed to revisit and broaden our understanding of the reaction mechanism involved in the (3 + 2)-cycloadditions of triflatophosphanes. In a previous study, we proposed that the dipolar cycloaddition reactions with alkynes (*cf.* Scheme 1, III) leading to compound **8** likely proceed *via* a concerted pathway.[15] However, due to the distinct nucleophilicity of nitriles, attributed to the free electron pair on the terminal nitrogen atom, a step-wise mechanism may be more appropriate. To investigate the energy barriers for the reaction of **24**[OTf] with acetonitrile, DFT calculations were performed at the PBE0-D3(COSMO)/def2-TZVP level of theory (Fig. 8). The results showed an overall Gibbs free energy of $\Delta G^{*} = -17.0$ kcal mol$^{-1}$ for the formation of **26a**$[OTf]_2$. Notably, the calculations reveal that the previously proposed concerted transition state pathway involves a high energy barrier through **TS′** (P–N 1.88 Å, C–N 2.05 Å). Alternatively, a stepwise mechanism appears more favourable, starting with the formation of an intermediate (**INT**) *via* **TS1** through nucleophilic substitution, with a low activation barrier of 2.7 kcal mol$^{-1}$. This initial step is exergonic by 13.6 kcal mol$^{-1}$. The subsequent ring closure proceeds through a second transition state (**TS2**)

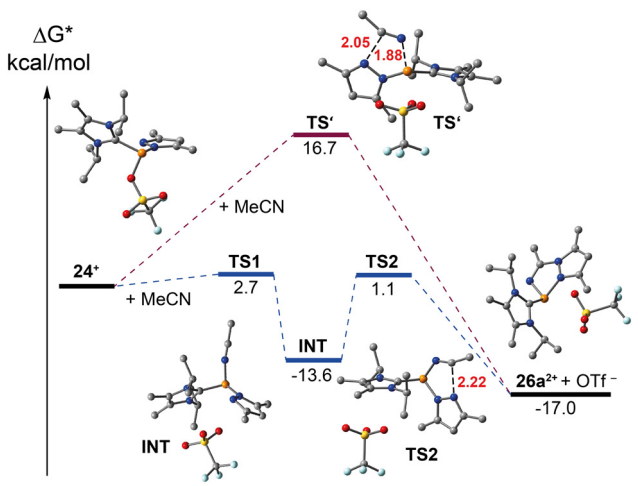


**Fig. 8** Gibbs free energies (in kcal mol$^{-1}$ at 298.15 K) of intermediates and transition states predicted for the (3 + 2)-cycloaddition of $\mathbf{24}^{+}$ with acetonitrile; PBE0-D3/def2-TZVP optimized geometries and energies; distances in Å.

with a moderate activation barrier of 14.6 kcal mol$^{-1}$, culminating in the formation of **26**[OTf]$_2$. Overall, these computational studies suggest that a stepwise reaction mechanism is energetically preferred when the dipolarophile features a nucleophilic moiety.

### 1,3-Dipolar cycloadditions of 24[OTf] with carbonyl compounds and protic substrates

We found that **24**[OTf] did not undergo selective reactions with various carbonyl compounds such as ketones and aldehydes, and attempts with alkynes were also unsuccessful (see ESI section 2.7†).

However, when **24**[OTf] was reacted with substrates like 4-bromphenylisocyanate, successful cycloaddition occurred, leading to the formation of triazaphospholium salt **27**[OTf]$_2$. Using naphthylisothiocyanate as the dipolarophile yielded thiatriazaphosphole **28**[OTf]$_2$ (Scheme 9). Notably, these reactions showed different regioselectivities as displayed in Scheme 9. In **28**$^{2+}$, the isothiocyanate reacted with the C=S double bond as the dipolarophile, while in **27**$^{2+}$, the C=N double bond participates in the ring formation. Single crystals of **27**[OTf]$_2$ and **28**[OTf]$_2$ were analysed by SC-XRD and the molecular structures of **27**$^{2+}$ and **28**$^{2+}$ are depicted in Fig. 9. **27**$^{2+}$ shows a planar diazaphospholium ring with a comparable P–N bond length (**27**$^{2+}$: P1–N1 1.735(2)) as in **26a**$^{2+}$ (P1–N1 1.7002(14)). The N1–C2 bond length however is elongated (**27**$^{2+}$: N1–C2 1.370(3), **26a**$^{2+}$: N1–C2 1.277(2)) due to the limited electron delocalization in **27**$^{2+}$. The molecular structure of **28**$^{2+}$ is closely comparable to that of **19**$^{2+}$, with a similar P–S bond length (**28**$^{2+}$: P1–S1 2.1212(8), **19**$^{2+}$: P1–S1 2.1328(5)).

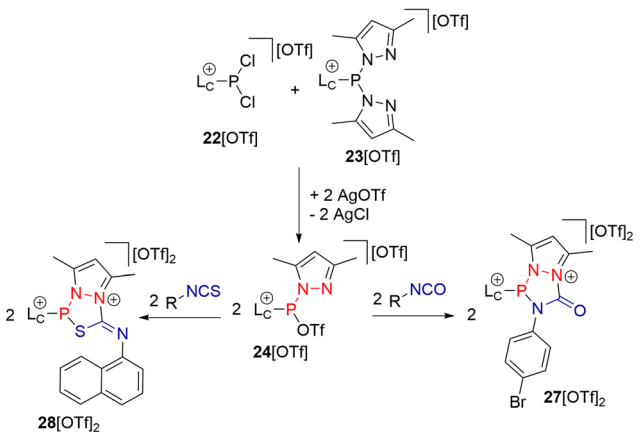


**Scheme 9** Reactions of *in situ* prepared **24**[OTf] with 4-bromphenylisocyanate and naphthylisothiocyanate.

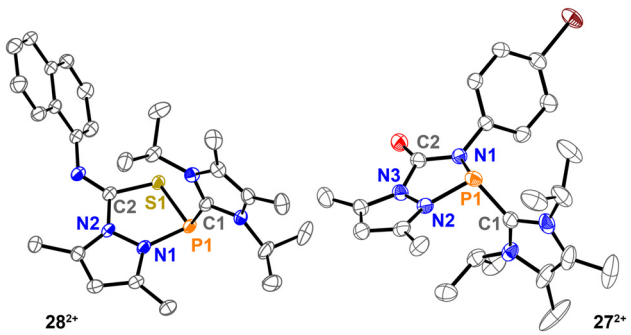


**Fig. 9** Molecular structures of **27**$^{2+}$ in **27**[OTf]$_2$·2CH$_2$Cl$_2$, and **28**$^{2+}$ in **28**[OTf]$_2$. (hydrogen atoms, solvate molecules, and anions are omitted for clarity; thermal ellipsoids are displayed at 50% probability). Selected bond lengths in Å and angles in (°): **27**$^{2+}$: P1–C1 1.819(3), P1–N1 1.735(2), P1–N2 1.765(2), N2–N3 1.363(3), N3–C2 1.433(3), N1–C2 1.370(3), C1–P1–N1 104.52(12), C1–P1–N2 101.74(12), N1–P1–N2 86.60(11), N3–N2–P1–N1 7.85(17); **28**$^{2+}$: P1–C1 1.833(3), P1–S1 2.1212(8), P1–N1 1.786(3), N1–N2 1.372(3), N2–C2 1.428(4), C1–S1 1.781(3), C1–P1–N1 101.81(12), C1–P1–S1 106.20(8), N1–P1–S1 90.42(8), N2–N1–P1–S1 3.53(19).

## Conclusions

In this study, we successfully expanded our cycloaddition protocol to various dipolarophiles, demonstrating the versatility of our methodology. We showed that *in situ* generated 1,3-dipolar triflatophosphanes readily react with nitriles, forming dizaphospholium salts **9a–f**[OTf]$_2$. These azaphospholium salts can be reduced irreversibly to neutral diazaphospholes, as evidenced by electrochemical examinations. The reduction reactions with $KC_8$ yielded diazaphospholes **14**, **16**, and **17**, offering a novel synthetic pathway to access diazaphospholes. We also explored the photophysical properties of these compounds, comparing them with analogous azaphospholes. Additionally, we demonstrated the selectivity of our approach by employing (thio) ketones as dipolarophiles, leading to the formation of oxazaphospholium salts **18a,b**[OTf]$_2$ and the thiazaphospholium salt **19**[OTf]$_2$. Remarkably, using phosphaalkene MesP=CPh$_2$, we obtained the unusual azadiphospholium salt **20**[OTf]$_2$.

Furthermore, by substituting the nucleophilic moiety from pyridine to pyrazole, triflatophosphane **24**[OTf] was synthesized and structurally characterized by SC-XRD. This compound exhibits similar reactivity towards nitriles, yielding triazaphospholium salts **26a–f**[OTf]$_2$. Quantum chemical calculations revealed that the reaction mechanism is step-wise, in contrast to the concerted mechanism observed with alkynes. While **24**[OTf] was unreactive towards (thio)ketones, it readily underwent a cycloaddition reaction with iso(thio)cyanates, demonstrating different regioselectivity depending on the chosen dipolarophile.

In summary, the cycloaddition scheme presented here serves as a strong foundation for further development of 1,3-dipolar cycloaddition reactions using phosphorus-based dipoles, a class with few known examples. This work opens new avenues for the synthesis of diverse heterocyclic ring systems, expanding the synthetic chemistry toolbox.

## Author contributions

J. F., K. S., and J. J. W. conceptualized the study; J. F. conducted the experiments and optimized the syntheses, isolations, and purifications; M. F. assisted with the syntheses;

J. H. conducted the electrochemical investigation; A. B. and A. F. were responsible for mechanistic studies; S. S. conducted the material simulations; R. H. conducted spectroscopic measurements; J. F., F. H., and J. J. W. were responsible for X-ray data collection and refinement; K. S. and J. J. W. conceived, oversaw, and directed the project; J. F., K. S., and J. J. W. prepared the initial draft of the paper; A. F., S. R., and J. J. W. secured funding. All authors contributed to data analysis, manuscript editing, and discussion.

## Data availability

The data supporting this article have been included as part of the ESI.† Crystallographic data for the structures reported in this paper have been deposited at the Cambridge Crystallographic Data Centre under the deposition number 2406453–2406470.†

## Conflicts of interest

There are no conflicts to declare.

## Acknowledgements

This work was supported by the German Science Foundation (DFG, WE 4621/6-1) and the European Union (R.H. acknowledges funding through project PNIRED, no. 101068895). A.F. thanks the MICIU/AEI of Spain (project PID2020-115637GB-I00 FEDER funds) for financial support. J.F. thanks the Graduate Academy of TU Dresden for financial support. S.S. thanks the Center for Information Services and High Performance Computing (ZIH) at TU Dresden for the use of computational facilities. Philipp Lange is acknowledged for performing elemental analyses. TU Dresden is also thanked for financial support.

## References

1 R. Huisgen, 1,3-Dipolar Cycloadditions. Past and Future, *Angew. Chem., Int. Ed. Engl.*, 1963, **2**, 565.

2 (*a*) M. Breugst and H.-U. Reissig, The Huisgen Reaction: Milestones of the 1,3-Dipolar Cycloaddition, *Angew. Chem., Int. Ed.*, 2020, **59**, 12293; (*b*) V. V. Rostovtsev, L. G. Green, V. V. Fokin and K. B. Sharpless, A Stepwise Huisgen Cycloaddition Process: Copper(I)-Catalyzed Regioselective "Ligation" of Azides and Terminal Alkynes, *Angew. Chem., Int. Ed.*, 2002, **41**, 2596.

3 (*a*) D. A. Bilodeau, K. D. Margison, M. Serhan and J. P. Pezacki, Bioorthogonal Reactions Utilizing Nitrones as Versitle Dipoles in Cycloaddition Reactions, *Chem. Rev.*, 2021, **121**, 6699; (*b*) D. Cantillo, B. Gutmann and C. O. Kappe, Mechanistic Insights on Azide-Nitrile Cycloadditions: On the Dialkyltin Oxide-Trimethylsilyl Azide Route and a New Vilsmeier-Haack-Type Organocatalyst, *J. Am. Chem. Soc.*, 2011, **133**, 4465; (*c*) T. Deb, J. Tu and R. M. Franzini, Mechanisms and Substituent Effects of Metal-Free Bioorthogonal Reactions, *Chem. Rev.*, 2021, **121**, 6850; (*d*) Z. P. Demko and K. B. Sharpless, A Click Chemistry Approach to Tetrazoles by Huisgen 1,3-Dipolar Cycloaddition: Synthesis of 5-Sulfonyl Tetrazoles from Azides and Sulfonyl Cyanides, *Angew. Chem., Int. Ed.*, 2002, **41**, 2110; (*e*) R. Huisgen, G. Szeimies and L. Möbius, 1.3-Dipolare Cycloadditionen, XXXII. Kinetik der Additionen organischer Azide an CC-Merfachbindungen, *Chem. Ber.*, 1967, **100**, 2494; (*f*) G. S. Kumar and Q. Lin, Light-Triggered Click Chemistry, *Chem. Rev.*, 2021, **121**, 6991; (*g*) J. C. Jewett and C. R. Bertozzi, Cu-free click cycloaddition reactions in chemical biology, *Chem. Soc. Rev.*, 2010, **39**, 1272; (*h*) M. Meldal and C. W. Tornøe, Cu-Catalyzed Azide-Alkyne Cycloaddition, *Chem. Rev.*, 2008, **108**, 2952; (*i*) C. G. Neochoritis, T. Zhao and A. Dömling, Tetrazoles via Multicomponent Reactions, *Chem. Rev.*, 2019, **119**, 1970; (*j*) K. Porte, M. Riomet, C. Figliola, D. Audisio and F. Taran, Click and Bio-Orthogonal Reactions with Mesoionic Compounds, *Chem. Rev.*, 2021, **121**, 6718; (*k*) K. Li, D. Fong, E. Meichsner and A. Adronov, A Survey of Strain-Promoted Azide-Alkyne Cycloaddition in Polymer Chemistry, *Chem. – Eur. J.*, 2021, **27**, 5057.

4 (*a*) T. Horneff, S. Chuprakov, N. Chernyak, V. Gevorgyan and V. V. Fokin, Rhodium-Catalyzed Transannulation of 1,2,3-Triazoles with Nitriles, *J. Am. Chem. Soc.*, 2008, **130**, 14972; (*b*) H. M. Davies and K. R. Romines, Directs synthesis of furans by 3 + 2 cycloaddtions between rhodium(II) acetate stabilized carbenoids and acetylenes, *Tetrahedron*, 1988, **44**, 3343.

5 (*a*) M. Stępień, E. Gońka, M. Żyła and N. Sprutta, Heterocyclic Nanographenes and Other Polycyclic Heteroaromatic Compounds: Synthetic Routes, Properties, and Applications, *Chem. Rev.*, 2017, **117**, 3479; (*b*) M. P. Duffy, W. Delaunay, P.-A. Bouit and M. Hissler, π-Conjugated phospholes and thier incorporation into devices: components with a great deal of potential, *Chem. Soc. Rev.*, 2016, **45**, 5296.

6 R. K. Bansal, K. Karaghiosoff and A. Schmidpeter, Anellated heterophospholes, *Tetrahedron*, 1994, **50**, 7675.

7 (*a*) E. Yue, L. Dettling, J. A. W. Sklorz, S. Kaiser, M. Weber and C. Müller, Au(I)-mediated $N_2$-elimination from triazaphospholes: a one-pot synthesis of novel $N_2P_2$-heterocycles, *Chem. Commun.*, 2021, **58**, 310; (*b*) L. Dettling, M. Papke, J. A. W. Sklorz, D. Buzsáki, Z. Kelemen, M. Weber, L. Nyulászi and C. Müller, A new access to diazaphospholes via cycloaddition cycloreversion reactions on triazaphospholes, *Chem. Commun.*, 2022, **58**, 7745.

8 W. Rösch and M. Regitz, [3 + 2]-Cycloaddition Reactions of a Stable Phosphaalkyne-Transition from Singly and Doubly Coordinated Phosphorus, *Angew. Chem., Int. Ed. Engl.*, 1984, **23**, 900.

9 U. Bergsträßer, A. Hoffmann and M. Regitz, A new access to phosphaindolizines by [3 + 2] cycloaddition of azomethine ylides onto phosphaalkynes, *Tetrahedron Lett.*, 1992, **33**, 1049.

10 W. Liang, K. Nakajima, K. Sakata and Y. Nishibayashi, Copper-Catalyzed [3 + 2] Cycloaddition Reactions of Isocyanoacetates with Phosphaalkynes to Prepare 1,3-Azaphospholes, *Angew. Chem., Int. Ed.*, 2019, **58**, 1168.

11 S. Hauer, J. Reitz, T. Koike, M. M. Hansmann and R. Wolf, Cycloadditions of Diazoalkenes with $P_4$ and tBuCP: Access to Diazaphospholes, *Angew. Chem., Int. Ed.*, 2024, e202410107.

12 W. J. Transue, A. Velian, M. Nava, M.-A. Martin-Drumel, C. C. Womack, J. Jiang, G.-L. Hou, X.-B. Wang, M. C. McCarthy, R. W. Field and C. C. Cummins, A Molecular Precursor to Phosphaethyne and Ist Application in Synthesis of the Aromatic 1,2,3,4-Phostriazolate Anion, *J. Am. Chem. Soc.*, 2016, **138**, 6731.

13 C.-X. Guo, K. Schwedtmann, J. Fidelius, F. Hennersdorf, A. Dickschat, A. Bauzá, A. Frontera and J. J. Weigand, Bifunctional Fluorophosphonium Triflates as Intramolecular Frustrated Lewis Pairs: Reversible $CO_2$ Sequestration and Binding of Carbonyls, Nitriles and Acetylenes, *Chem. – Eur. J.*, 2021, **27**, 13709.

14 R. Streubel, H. Wilkens, A. Ostrowski, C. Neumann, F. Ruthe and P. G. Jones, Formation of 2H-1,2-Azaphosphole Tungsten Complexes by Trapping Reactions of Nitrilium Phosphane Ylide Complexes, *Angew. Chem., Int. Ed. Engl.*, 1997, **36**, 1492.

15 J. Fidelius, K. Schwedtmann, S. Schellhammer, J. Haberstroh, S. Schulz, R. Huang, M. C. Klotzsche, A. Bauzá, A. Frontera, S. Reineke and J. J. Weigand, Convenient access to p-conjugated 1,3-azaphospholes from alkynes via [3 + 2]-cycloaddition and reductive aromatization, *Chem*, 2024, **10**, 644.

16 J. J. Weigand, K.-O. Feldmann and F. D. Henne, Carbene-Stabilzed Phosphorus(III)-Centered Cations $[LPX_2]^+$ and $[L_2PX]^{2+}$ (L = NHC; X = Cl, CN, $N_3$), *J. Am. Chem. Soc.*, 2010, **132**, 16321.

17 V. Kremláček, J. Hyvl, W. Y. Yoshida, A. Růžička, A. L. Rheingold, J. Turek, R. P. Hughes, L. Dostál and M. F. Cain, Heterocycles Derived from Generating Monovalent Pnictogens within NCN Pincers and Bidentate NC Chelates: Hypervalency vs. Bell-Clappers vs. Static Organometallics, *Organometallics*, 2018, **37**, 2481.

18 P. Royla, K. Schwedtmann, Z. Han, J. Fidelius, D. P. Gates, R. M. Gomila, A. Frontera and J. J. Weigand, Cationic Phosphinidene as a Versatile $P_1$ Building Block: $[LC\text{-}P]^+$ Transfer from Phosphonio-Phosphanides $[LC\text{-}P\text{-}PR_3]^+$ and Subsequent LC Replacement Reactions (LC = N-Heterocyclic Carbene), *J. Am. Chem. Soc.*, 2023, **145**, 10364.

19 M. Baudler, G. Reuschenbach, D. Koch and B. Carlsohn, Beiträge zur Chemie des Phosphors, 88. 1,2,3-Triphenyl-1,3-bis(trimethylsilyl)triphosphan, *Chem. Ber.*, 1980, **113**, 1264.

20 C. Taube, K. Schwedtmann, M. Noikham, E. Somsook, F. Hennersdorf, R. Wolf and J. J. Weigand, P-P Condensation and P-N/P-P Bond Metathesis: Facile Synthesis of Cationic Tri- and Tetraphosphanes, *Angew. Chem., Int. Ed.*, 2020, **59**, 3585.

21 K.-O. Feldmann and J. J. Weigand, P-N/P-P bond metathesis for the synthesis of complex polyphosphanes, *J. Am. Chem. Soc.*, 2012, **134**, 15443.

22 (*a*) C. A. Caputo, J. T. Price, M. C. Jennings, R. McDonald and N. D. Jones, N-Heterocyclic phosphenium cations: synthesis and cycloaddition reactions, *Dalton Trans.*, 2008, 3461; (*b*) A. Dumitrescu, H. Gornitzka, W. W. Schoeller, D. Bourissou and G. Bertrand, A Crystalline Phosphenium Salt Featuring the Electron-Withdrawing 2,6-Bis(trifluoromethyl)phenyl Group, *Eur. J. Inorg. Chem.*, 2002, 1953; (*c*) S. Yogendra, F. Hennersdorf, A. Bauzá, A. Frontera, R. Fischer and J. J. Weigand, Carbodiphosphorane mediated synthesis of a triflyloxyphosphonium dication and its reactivity towards nucleophiles, *Chem. Commun.*, 2017, **53**, 2954.

23 (*a*) R. Szűcs, P.-A. Bouit, M. Hissler and L. Nyulászi, Edge modification of PAHs: the effect of embedded heterocycles on the aromaticity pattern, *Struct. Chem.*, 2015, **26**, 1351; (*b*) L. Nyulaszi, T. Veszpremi, J. Reffy, B. Burkhardt and M. Regitz, Electronic structure and aromaticity of azaphospholes, *J. Am. Chem. Soc.*, 1992, **114**, 9080.